SHOCK, Vol. 60, No. 1, pp. 1–10, 2023

OPEN

CONSTRUCTION OF SEPSIS DIAGNOSTIC MODELS AND IDENTIFICATION OF MACROPHAGE SUBPOPULATIONS BASED ON PYROPTOSIS-RELATED GENES

Zefang Sun,*† Tao Zhang,*† Caihong Ning,*† Dingcheng Shen,*† Wenwu Pei,†‡ Rui Zhou,† Shuai Zhu,*† and Gengwen Huang*†

**Department of Pancreatic Surgery, General Surgery, Xiangya Hospital, Central South University, Changsha, China; and †National Clinical Research Center for Geriatric Disorders, Xiangya Hospital, Central South University, Changsha, China; and ‡Department of Gastrointestinal Surgery, General Surgery, Xiangya Hospital, Central South University, Changsha, China*

Received 2 Dec 2022; first review completed 3 Jan 2023; accepted in final form 2 Apr 2023

ABSTRACT—**Background:** Numerous studies have shown that pyroptosis is associated with sepsis progression, which can lead to dysregulated host immune responses and organ dysfunction. Therefore, investigating the potential prognostic and diagnostic values of pyroptosis in patients with sepsis is essential. **Methods:** We conducted a study using bulk and single-cell RNA sequencing (scRNA-seq) from the Gene Expression Omnibus database to examine the role of pyroptosis in sepsis. Univariate logistic analysis, least absolute shrinkage, and selection operator regression analysis were used to identify pyroptosis-related genes (PRGs), construct a diagnostic risk score model, and evaluate the selected genes' diagnostic value. Consensus clustering analysis was used to identify the PRG-related sepsis subtypes with varying prognoses. Functional and immune infiltration analyses were used to explain the subtypes' distinct prognoses, and scRNA-seq data were used to differentiate immune-infiltrating cells and macrophage subsets and study cell-cell communication. **Results:** A risk model was established based on 10 key PRGs (*NAIP*, *ELANE*, *GSDMB*, *DHX9*, *NLRP3*, *CASP8*, *GSDMD*, *CASP4*, *APIP*, and *DPP9*), of which four (*ELANE*, *DHX9*, *GSDMD*, and *CASP4*) were associated with prognosis. Two subtypes with different prognoses were identified based on the key PRG expressions. Functional enrichment analysis revealed diminished nucleotide oligomerization domain–like receptor pathway activity and enhanced neutrophil extracellular trap formation in the subtype with a poor prognosis. Immune infiltration analysis suggested a different immune status between the two sepsis subtypes, with the subtype with a poor prognosis exhibiting stronger immunosuppression. The single-cell analysis identified a macrophage subpopulation characterized by gasdermin D (GSDMD) expression that may be involved in pyroptosis regulation, which was associated with the prognosis of sepsis. **Conclusion:** We developed and validated a risk score for sepsis identification based on 10 PRGs, four of which also have potential value in the prognosis of sepsis. We identified a subset of gasdermin D macrophages associated with poor prognosis, providing new insights into the role of pyroptosis in sepsis.

KEYWORDS—Sepsis; pyroptosis; diagnosis; prognosis; scRNA-seq; bulk RNA-seq

INTRODUCTION

Sepsis is a life-threatening organ dysfunction caused by an exaggerated systemic inflammatory response to different infections (1). It is prevalent in patients admitted to intensive care units and has an unacceptably high mortality rate. Infections trigger inflammatory reactions that induce cytokine release, leading to multiorgan system failure (2,3). Sepsis is characterized by sustained excessive inflammation and immune suppression (4), and although there has been a significant increase in our understanding of its key mechanisms, its 30-day mortality rate remains high at 34.7% (5). Early diagnosis and prognosis determination are critical for its treatment (6,7), making it essential to explore early diagnosis and prognosis-related signatures in patients with sepsis.

Pyroptosis is a recently discovered atypical form of programmed cell death that occurs because of an inflammatory response, depending on the classic pathway of caspase-1 and the noncanonical pathway of caspase-11 in mice or the ortholog caspases 4 or 5 in humans (8,9). Activated caspases cleave the gasdermin D (GSDMD) protein, which produces an N-terminal domain, perforates the cell membrane, and results in pyroptosis. Excessive pyroptosis activation has been implicated in various human diseases and conditions, including sepsis. Altered pyroptosis-related gene (PRG) expression plays a critical role in triggering and developing sepsis (10,11), and their dysregulation has also been found to participate in the pathogenesis of multiple organ system failures (12). Activated GSDMD triggers macrophage pyroptotic cell death, leading to increased septic lethality (13). Caspase-11–dependent pyroptosis contributes to endotoxemic lethality and bacterial sepsis (14). Accumulating evidence has demonstrated the major role of many single PRGs in sepsis, including their mechanisms and relevant targets of

Address reprint requests to Gengwen Huang, Ph.D., Department of Pancreatic Surgery, General Surgery, Xiangya Hospital, Central South University, Changsha, No.87 Xiangya Road, Changsha, Hunan, 410000, China. E-mail: huanggengwen@csu.edu.cn; Co-correspondence: Shuai Zhu, Ph.D., Department of Pancreatic Surgery, General Surgery, Xiangya Hospital, Central South University, Changsha, No.87 Xiangya Road, Changsha, Hunan, 410000, China. E-mail: zhushuai@csu.edu.cn

Z.S. and T.Z. contributed equally to this work.

This work was supported by the National Natural Science Foundation of China (81802450) and the Natural Science Foundation of Hunan Province (2020JJ4133, 2021JJ31135).

The authors report no conflicts of interest.

Z.S. and S.Z. designed the study and analyzed the data. Z.S. and Z.T. drafted the manuscript. W.P., R.Z., S.Z., and D.S. revised the manuscript. S.Z. and G.H. supervised the study and contributed to manuscript revision, with contributions from all other authors. All the authors have read and approved the final version of the manuscript.

The GSE65682, GSE57065, GSE95233, and GSE167363 data sets were downloaded from the GEO database (https://www.ncbi.nlm.nih.gov/geo/query/acc.cgi?acc=GSE65682, https://www.ncbi.nlm.nih.gov/geo/query/acc.cgi?acc=GSE57065, https://www.ncbi.nlm.nih.gov/geo/query/acc.cgi?acc=GSE95233, and https://www.ncbi.nlm.nih.gov/geo/query/acc.cgi?acc=GSE167363). The scRNA-seq data set, GSE167363, was downloaded from the GEO database (https://www.ncbi.nlm.nih.gov/geo/query/acc.cgi?acc=GSE167363).

Supplemental digital content is available for this article. Direct URL citation appears in the printed text and is provided in the HTML and PDF versions of this article on the journal's Web site (www.shockjournal.com).

DOI: 10.1097/SHK.0000000000002137

pyroptosis in sepsis (15–17). However, an integrated signature can provide a comprehensive analysis of PRGs in sepsis, thereby advancing our understanding of the mechanisms underlying sepsis.

This study identified the expression signatures of 10 PRGs using bulk RNA-sequencing (RNA-seq) and developed and validated a new pyroptosis-related risk score model for the identification of sepsis. The study also described the different pyroptosis states of sepsis samples and their relationship with prognosis, analyzed and studied immune cell infiltration and related signaling pathways, and attempted to explain the mechanisms underlying the different prognoses between subtypes. Furthermore, the study explored the expression patterns of PRGs in the early stages of sepsis using single-cell RNA sequencing (scRNA-seq). The results identified a macrophage subpopulation characterized by GSDMD expression, which may be associated with prognosis. These results could potentially provide new insights into the role of pyroptosis in sepsis and its diagnosis and prognosis.

MATERIALS AND METHODS

Data acquisition and processing

A series of data sets from the Gene Expression Omnibus (GEO) database were used in this study. GSE65682, comprising 479 patients with sepsis with complete clinical data and 42 healthy controls, was used to analyze the expression patterns of PRGs and construct a pyroptosis-related diagnostic model. The GSE95233 and GSE57065 data sets were used to verify the efficacy of the diagnostic model. The GSE49756 data set was used to explore PRG expression in neutrophils during sepsis. Gene probes were converted to gene symbols using the corresponding annotation profiles in each data set. We used the "limma" package in R sofware: https://www.r-project.org/ to normalize all gene expression values by quartiles and generate normally distributed expression values. For multiple identical probes, finite gene expression values were determined by calculating the average expression values. Detailed information is provided in Supplemental Digital Content (Supplementary Table S1, http://links.lww.com/SHK/B698). Because the GEO database is publicly available, ethical approval was not required for this study.

The single-cell sequencing data set GSE167363 was used to explore the immune landscape and PRG expression during sepsis. Data analysis was performed in R using Seurat v4 (18). Cells with <100 or >5,000 transcripts were excluded from the analysis to filter out empty droplets, low-quality cells, and multiplets. In addition, cells of poor quality, recognized as cells with >10% of their transcripts originating from mitochondrial genes, were excluded from the downstream analysis. The whole workflow for the bioinformatics analysis is illustrated in Supplemental Digital Content (Supplementary Fig. S1, http://links.lww.com/SHK/B693).

Localization and interaction of PRGs

Pyroptosis-related genes were downloaded from the Molecular Signatures Database (MSigDB) (https://www.gsea-msigdb.org/gsea/msigdb/cards/GOBP_PYROPTOSIS.html). The hg38 genome file (https://hgdownload.soe.ucsc.edu/goldenPath/hg38/bigZips/genes/) was downloaded from the UCSC Genome Browser to obtain genome location coordinates. The PRGs were extracted according to the pyroptosis (Gene Ontology [GO], 0070269) of the GO Biological Process 2021 database. R Circos: https://github.com/cran/RCircos V1.2.1 was used to visualize the genomic structure of the PRGs. The relationships between PRGs were imported into STRING (https://string-db.org) to analyze the protein-protein interaction network.

Differential analysis and logistic regression of disease-associated PRGs

Differential expression analysis was performed using the limma package. Genes with a |log2 (fold change)| ≥0.5 and P values ≤0.05 were identified as differentially expressed genes (DEGs). A correlation analysis was performed to determine the relevance of PRGs in the pyroptosis pathway. Pyroptosis-related genes, age, and sex were used to perform a univariate logistic regression analysis to evaluate the diagnostic value. Factors with P values >0.05 continued to be used for least absolute shrinkage and selection operator (LASSO) regression by the "glmnet" package. The penalty coefficient λ was determined by using the minimal criteria, and candidate genes with a regression coefficient unequal to zero were included. Factors screened by logistic LASSO regression were considered significant and were used to construct a multiple logistic regression. The risk score of each patient was calculated according to the following formula: risk score = ∑coefficient PRG × gene expression value of PRG. The receiver operating characteristic (ROC) curves were used to test the diagnostic efficacy of multiple logistic regression using the "ROCR" package. The Kaplan-Meier survival curves were constructed to determine the relationship between significant factors and survival status. We used the "survival R" package and the "survminer R" package to produce the Kaplan-Meier survival curves.

Identification of molecular subtypes mediated by PRGs

Consensus clustering is a common subtype classification method that divides samples into several subtypes based on different omics data sets to identify new disease subtypes. The Partition Around Medoids algorithm with Euclidean distance was used, and the samples were iterated 1,000 times. To identify the optimal clusters, the number of clusters was determined by the relative change in the cumulative distribution function (CDF) of the consensus cluster and the area under the CDF curve from $k = 2$ to 5. The Kaplan-Meier curves were used to analyze the differences in the survival status of the different subtypes.

Functional enrichment analysis and immune infiltration analysis

Based on the same criteria, we again used the limma package to screen for DEGs among sepsis subtypes. To explore the signaling pathways and biological functions associated with DEGs, we used the "clusterprofiler" package to perform the Kyoto Encyclopedia of Genes and Genomes and GO analyses of the differential genes. The immunoedeconv R package was used for immune-infiltrating cell analysis to quantify the relative proportion of immune cells. The composition of these immune cells in the different groups was compared using the Wilcoxon signed rank test. The "corrplot" package was used for evaluating the correlation relationship between PRGs and immune cells.

scRNA analysis for PRGs

The R package "Seurat" was used to analyze the scRNA-seq data. Gene expression measurements for each cell were normalized by the total number of transcripts in the cell multiplied by a default scale factor, and the normalized values were log-transformed ("LogNormalize" method). Following the Seurat workflow, for each replicate, the 2,000 most highly variable genes were identified using variance stabilizing transformation ("vst"). All conditions were integrated using the Seurat v4 approach. To avoid obtaining results fitted too closely to a particular data set and therefore possibly failing to fit additional data, 2,000 integration anchors were first found. These anchors are then used as inputs for the data set integration procedure. Clustering results were visualized using two-dimensional uniform manifold approximation and projection (19). Cell-cell interaction analysis was performed using the R package "CellChat." The R package CellChat requires gene expression data from cells as user input and models the probability of cell-cell communication by integrating gene expression with prior knowledge of the interactions between signaling ligands, receptors, and their cofactors. Secreted signaling and cell-cell contact in human databases were used. Circle diagrams were used to display the strength of the cell-cell communication networks from the target cell cluster to other cell clusters.

Statistical analysis

All statistical analyses were performed using R software (version 4.1.0) and R studio: https://cran.rstudio.com/ (version 1.2.5042). The Wilcoxon test was used to compare the gene expression level between sepsis patients and healthy individuals, and the composition of immune cells in different disease status and subgroups. Pearson chi-square test was applied to compare categorical variables. Univariate logistic-LASSO regression was used for candidate genes selection. The Kaplan-Meier method and log-rank test were used to compare the survival rate for different PRGs expression and subtype. Univariate and multivariate logistic regression analyses were used to assess the independent prognostic variables. A two-tailed P value <0.05 was considered statistically significant.

RESULTS

PRGs in sepsis

In the MSigDB database, 21 PRGs were detected. The PRGs were mapped to the human genome (Fig. 1A). We used STRING to analyze the protein-protein interaction network to study the interaction network between PRGs (Fig. 1B). The core proteins of this network were GSDMD, NLRP3, AIM2, ELANE, and caspases 1, 4, and 8, of which NLRP3-caspase 1/4-GSDMD is the canonical

pyroptosis pathway and ELANE was discovered to be the key gene in the neutrophil pyroptosis pathway. The analysis of differentially expressed PRGs in sepsis suggested that five PRGs were upregulated (*NAIP*, *NLRC4*, *ELANE*, *NLRP3*, and *AIM2*) ($P \leq 0.05$ and $\log_2FC \geq 0.5$), whereas seven genes were downregulated (*NLRP1*, *GSDMB*, *GZMA*, *GZMB*, *DHX9*, *CASP6*, and *CASP8*) ($P \leq 0.05$ and $\log_2FC \geq -0.5$) (Fig. 1, C and D; Supplemental Digital Content, Supplementary Fig. S4A, http://links.lww.com/SHK/B696), and nine genes were stable (Supplemental Digital Content, Table S3, http://links.lww.com/SHK/B699). Correlation analysis of the PRGs indicated a significant positive correlation between *GSDMD* and *CASP1/4* (Fig. 1, F and G).

Development of PRGs related risk model

A univariate logistic analysis was performed on the 21 PRGs, age, and sex. Among these factors, 17 PRGs (*NLRC4*, *NAIP*, *AIM2*, *ELANE*, *NLRP1*, *GZMA*, *GSDMB*, *DHX9*, *CASP6*, *NLRP3*, *CASP8*, *GSDMD*, *CASP4*, *CASP1*, *NLRP6*, *PYCARD*, *APIP*, and *DPP9*) and age factors ($P < 0.05$) were selected as candidate elements for LASSO analysis (Fig. 2A; Supplemental Digital Content, Supplementary Table S2, http://links.lww.com/SHK/B700). All 521 samples were randomly assigned to the training (n = 365) and validation (n = 156) sets in a ratio of 7:3. Based on the cross-validation results of the LASSO analysis (Fig. 2, B and C), 10 PRGs (*NAIP*, *ELANE*, *GSDMB*, *DHX9*, *NLRP3*, *CASP8*, *GSDMD*, *CASP4*, *APIP*, and *DPP9*) were considered valuable predictors of sepsis, and age factors were excluded. The ROC curve results suggested that the LASSO model performed well in the diagnosis of sepsis (Supplemental Digital Content, Supplementary Fig. S2, http://links.lww.com/SHK/B694). Finally, 10 PRGs were used to construct a risk model using multivariate logistic regression analysis (Fig. 2D). The risk score for each patient was calculated as

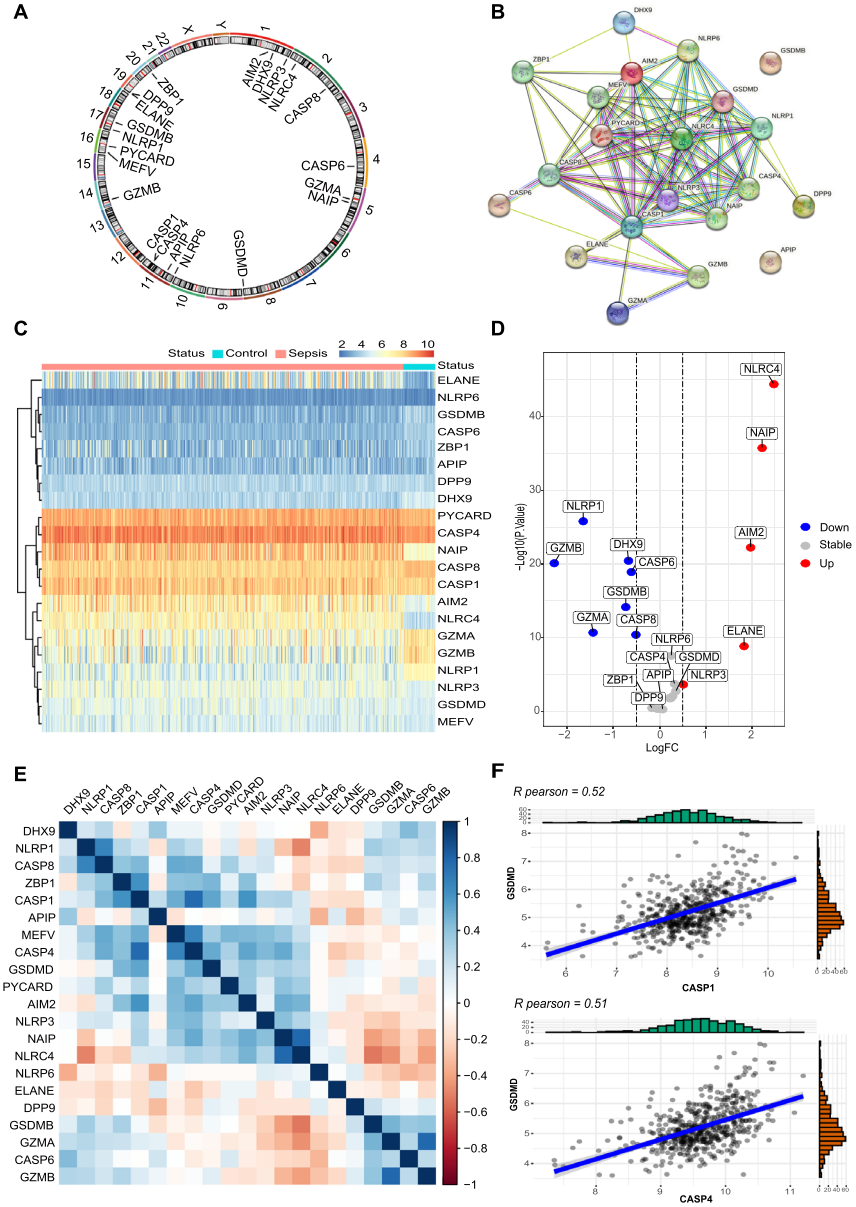

FIG. 1. **Location and differentially expressed analysis for PRGs**. (A) Genome location for PRGs. (B) The protein-protein interaction for PRGs. (C) The heat map and boxplot show the differential expression patterns of PRGs in sepsis. (D) The volcano map shows the upregulated or downregulated PRGs in sepsis compared with healthy controls. (E) Correlation analysis for PRGs in sepsis samples. (F) The scatter plot shows the correlation between GSDMD and CASP1/CASP4. PRG indicates pyroptosis-related genes.

follows: risk score = (−10.53 × DPP9) + (−7.55 × CASP8) + (−1.29 × NAIP) + (−3.51 × APIP) + (3.28 × GSDMB) + (1.19 × CASP4) + (−0.04 × NLRP3) + (−1.51 × ELANE) + (8.12 × GSDMD) + (4.59 × DHX9). The area under the ROC curve indicated that the risk model based on the 10 PRGs had excellent performance in the identification of sepsis, indicating that these key PRGs play an essential role in the development of sepsis (Fig. 2E). Sepsis data sets (GSE57065 and GSE95233) were used to validate the diagnostic efficacy of the risk model. The area under the ROC curve of the two validation sets was 0.895 (GSE57065) and 0.837 (GSE95233), suggesting that the risk model had stable diagnostic efficacy (Fig. 2E). Indeed, according to the risk score distribution, the risk score was much higher in patients with sepsis than in normal controls (Fig. 2F). Furthermore, we analyzed the relationship between the 10 key PRGs and the prognosis of patients with sepsis, and the survival curves suggested that *CASP4*, *ELANE*, *GADMD*, and *DHX* were significantly associated with prognosis (Fig. 2G).

Identification of pyroptosis-related molecular subtypes

In the consensus clustering analysis, $k = 2$ was considered the optimal parameter based on the empirical CDF (Supplemental Digital Content, Supplementary Fig. S3, A and B, http://links.lww.com/SHK/B695). Sepsis samples were divided into two subtypes with significant differences in the key PRG expression (Fig. 3A). *ELANE* and *APIP* showed significantly higher expression in subtype

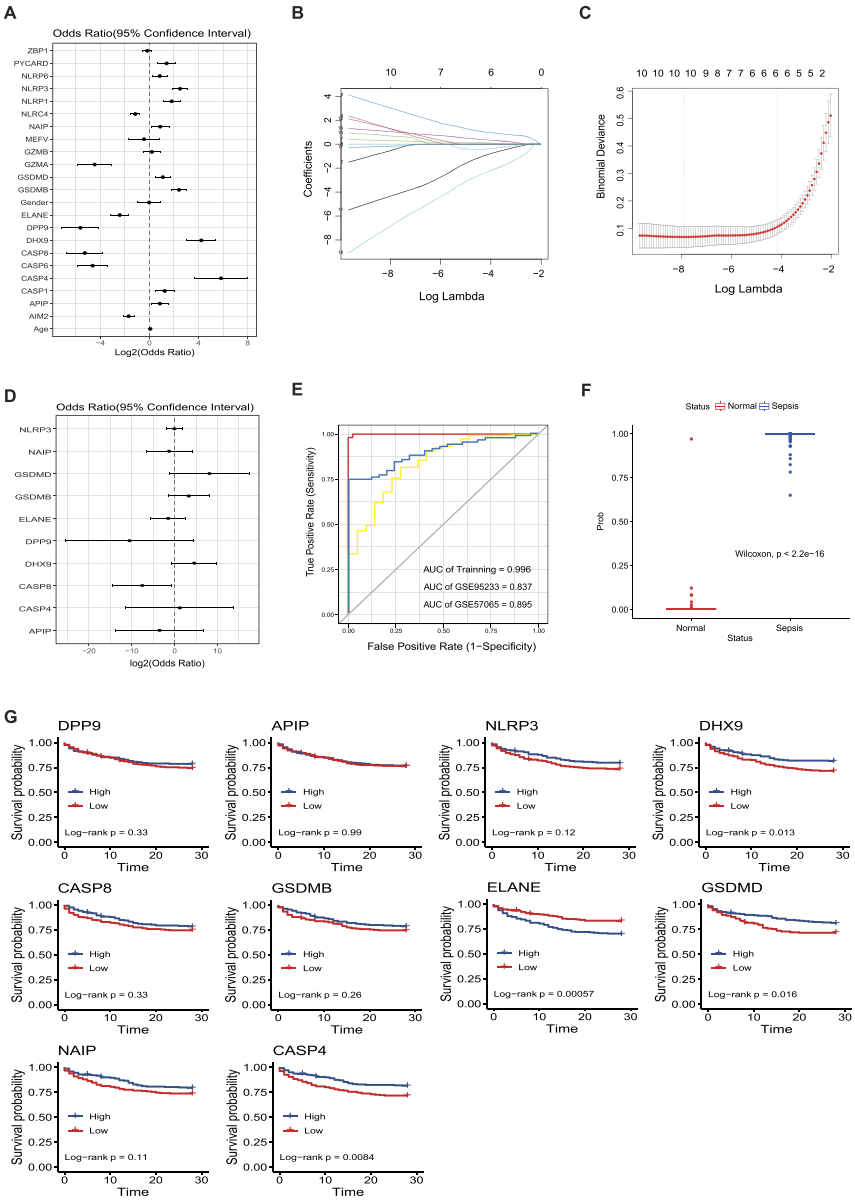

FIG. 2. **The development of risk models based on PRGs.** (A) A univariate logistic regression was performed to identify the association between PRGs and sepsis. (B) The LASSO regression minimum absolute shrinkage and LASSO coefficient distribution. (C) Ten-fold cross-validation for adjusting parameter selection in LASSO regression, where λ is the adjustment parameter. The partial likelihood deviation value is displayed, and the error bar represents SE. The vertical dashed line is drawn at its best value by the minimum criterion and the 1-SE criterion. (D) A multivariate logistic regression was used to confirm the univariate result. (E) The performance of the risk model for training data set and validation data set was shown by the ROC curve. (F) The distribution of risk scores between patients with sepsis and healthy controls. (G) Kaplan-Meier curves analysis of key PRGs expression for the survival of patients. PRG indicates pyroptosis-related genes; LASSO, least absolute shrinkage and selection operator; ROC, receiver operating characteristic; SE, standard error.

2, whereas *CASP4*, *CASP8*, *GSDMD*, *NLRP3*, and *NAIP* showed significantly lower expression (Fig. 3D; Supplemental Digital Content, Supplementary Fig. S4B, http://links.lww.com/SHK/B696). Patients with this subtype have a poorer prognosis than those with the first subtype (Fig. 3B). In total, 251 DEGs were identified between the two subtypes. A total of 205 genes were upregulated, and 46 genes were downregulated in subtype 2 (Fig. 3C). Based on these DEGs, we performed functional enrichment analysis, and the results showed that the upregulated DEGs were mainly associated with neutrophil extracellular trap (NET) formation and DNA replication and were involved in negative apoptotic regulation. The downregulated genes were mainly related to the nucleotide oligomerization domain (NOD)–like and cytokine receptor pathways (Fig. 3, E and F).

PRGs and the immune microenvironment

Furthermore, we evaluated the immune microenvironments of patients with sepsis and its subtypes. Immune infiltration analysis suggested that neutrophils comprised the majority of immune cells. Effector cells such as B and CD8+ T cells were reduced in the septic environment, and the proportion of Tregs increased, which is consistent with the landscape of immunosuppression in sepsis (Fig. 4A). In the immune landscape of the sepsis subtypes, subtype 2 had a higher proportion of Treg cells (Fig. 4C) and lower activity of all immune pathways, suggesting stronger immunosuppression (Fig. 4, B and D). The interaction heat map suggested that there was a correlation between the key PRG and various immune cells in sepsis, among which neutrophils and Tregs were closely related to the key PRG (Fig. 4E). The human leukocyte antigens (*HLA*)

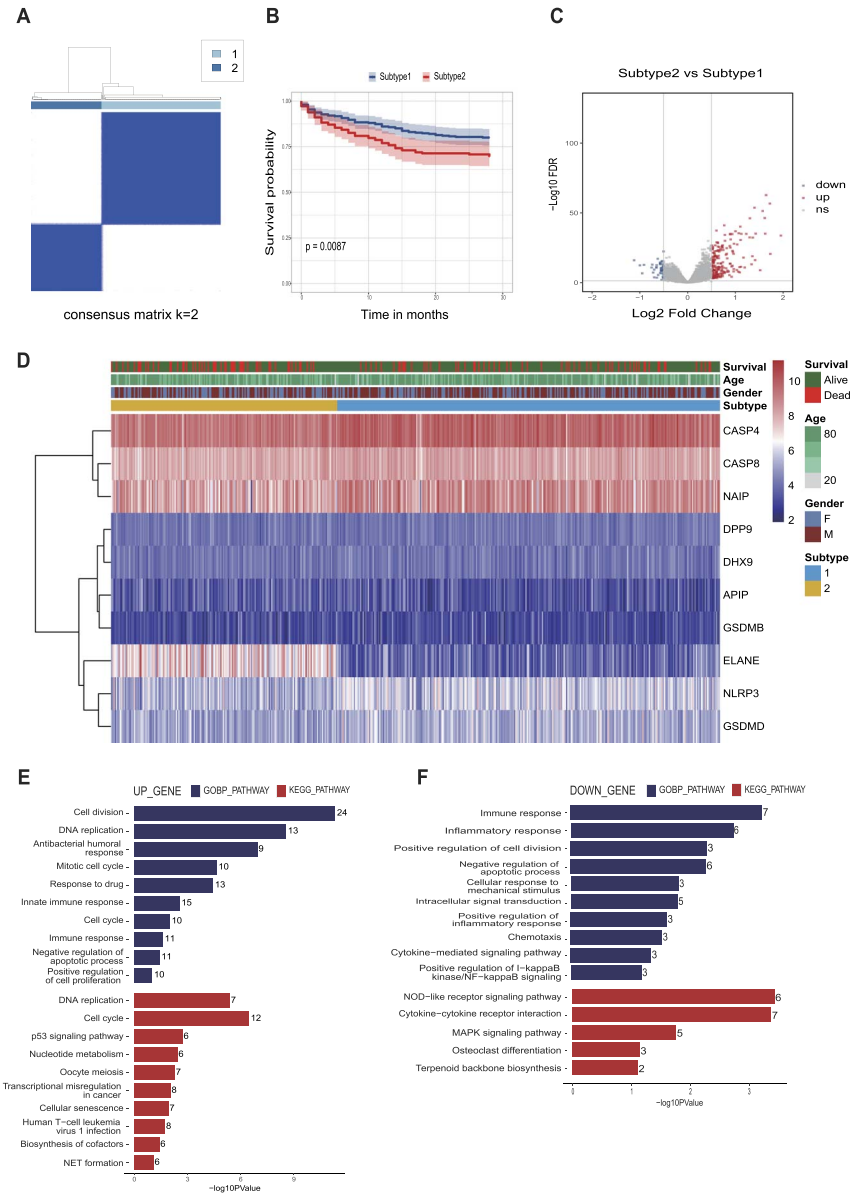

FIG. 3. **Identification of the PRG-based subtype.** (A) Non-NMF consensus analysis for $k = 2$. (B) Kaplan-Meier curves analysis for the survival of different subtypes. (C) The volcano map shows the DEGs upregulated or downregulated between subtypes 1 and 2. (D) Heat map for PRGs differentially expressed and its clinical manifestation between subtypes 1 and 2. (E, F) The GO items of biological processes and KEGG pathway analysis for DEGs in subtypes. NMF indicates negative matrix factorization; PRG, pyroptosis-related genes; GO, gene ontology; KEGG, Kyoto Encyclopedia of Genes and Genomes; DEG, differentially expressed gene.

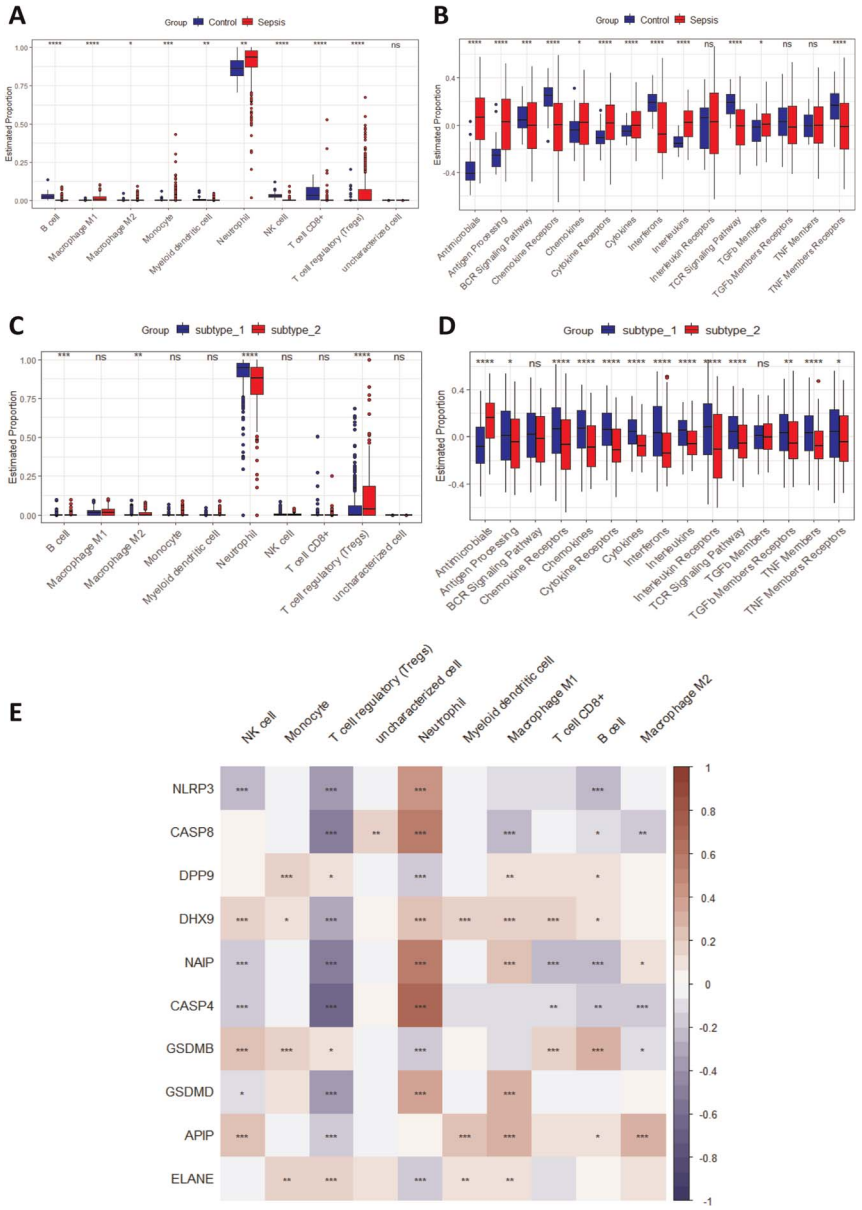

FIG. 4. **Immune infiltration landscape in PRG-based subtypes.** (A) Boxplots representing the PRGs expression levels between sepsis and control. (B) Boxplots for the common immune pathway between sepsis and control. (C) Boxplots representing the PRGs expression levels in clusters 1 and 2. (D) Boxplots for the common immune pathway in clusters 1 and 2. (E) The correlation between the selected 10 PRGs and the immune cells. *$P < 0.05$; **$P < 0.01$; ***$P < 0.001$. PRG indicates pyroptosis-related genes.

gene expression suggests that the HLA-DR isotype (HLA-DR) is downregulated during sepsis. Among these, HLA-DRA and HLA-DRB5 levels further decreased in the second subtype (Supplemental Digital Content, Supplementary Fig. S4, C and D, http://links.lww.com/SHK/B696).

Single-cell landscape for PRGs in sepsis

Peripheral blood mononuclear cell samples extracted from human peripheral blood were used to explore the expression patterns of PRGs during sepsis. Eight cell types were identified using specific markers (Fig. 5, A and B). Compared with healthy controls, B cells, Tregs, and CD8+ T cells decreased gradually, but macrophages and monocytes increased with the development of sepsis (Fig. 5C). Gene set enrichment analysis revealed that immune pathways, such as interferon α or γ and IL6-JAK-STAT3, and inflammatory pathways were significantly upregulated at the beginning of sepsis. However, 6 hours later, metabolism-related pathways, such as oxidative phosphorylation, cholesterol homeostasis, and reactive oxygen pathways, were activated, whereas the immune pathways were no longer enriched, suggesting that immune function was downregulated and metabolic disorders may occur in some cell metabolic pathways (Fig. 5D). Furthermore, we analyzed single-cell heat maps of the inflammatory and immune pathways. These results suggested that inflammatory reactions and immune pathways were gradually inactivated during sepsis (Fig. 5E; Supplemental Digital Content, Supplementary Fig. S5, http://links.lww.com/SHK/B697). The results of PRG's expression analysis indicated that PRG was mainly expressed in macrophages, CD4+ T, CD8+ T, and Treg cells. *ELANE*, *GSDMD*, and *NAIP* were significantly upregulated during sepsis (Fig. 5F), and the overall PRG expression gradually increased with sepsis progression (Fig. 5G). Also, a neutrophil expression-based analysis

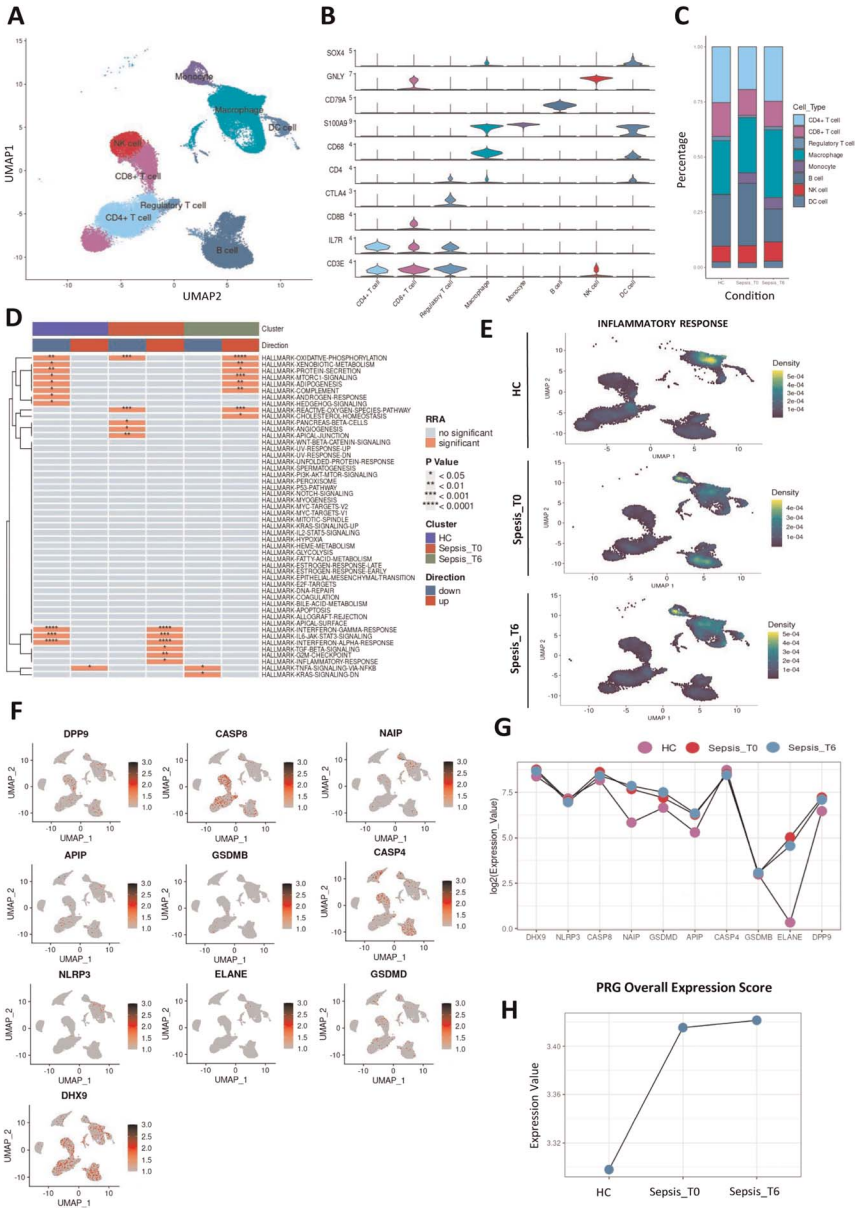

FIG. 5. **Single-cell RNA sequencing analysis for PRGs in sepsis.** (A) The UMAP plot of immune cell types. (B) A violin plot showing the cell-specific marker gene expressions. (C) The percentage bar plot displayed the immune cell composition in healthy controls and patients with sepsis, initially recognized and after 6 hours. (D) A pathway heat map based on the top 50 genes in healthy controls and patients with sepsis, initially recognized and after 6 hours. (E) Immune cell heat map for an inflammatory response in healthy controls and patients with sepsis, initially recognized and after 6 hours. (F) The UMAP plot of single PRG expression heat map in sepsis status. (G) The single PRG expression levels in healthy controls and patients with sepsis, initially recognized and after 6 hours. (H) The overall PRG expression levels in healthy controls and patients with sepsis, initially recognized and after 6 hours. UMAP indicates uniform manifold approximation and projection; PRG, pyroptosis-related genes.

showed that *ELANE* was upregulated during sepsis and even higher in patients with a poor prognosis (Supplemental Digital Content, Supplementary Fig. S4E, http://links.lww.com/SHK/B696).

Identification of GSDMD macrophages

Further cluster analysis classified the macrophages into seven classes (Fig. 6A). Each macrophage subgroup was annotated according to the cellular markers identified, and seven specific macrophage subgroups (GSDMD, LGALS2, GNLY, IGHM, MARCO, AREG, and STMN1) were identified (Fig. 6B). We compared the proportions of macrophage subgroups in healthy controls, sepsis t0, and sepsis t6 samples and found that the proportion of GSDMD macrophages increased progressively with the progression of sepsis and was present only in patients who died (Fig. 6, C and E). Enrichment analysis was performed to better understand the function of GSDMD macrophages. These results suggested that GSDMD macrophages were mainly involved in NOD-like receptor signaling, apoptosis, and viral infection pathways (Fig. 6D). Cell communication analysis showed that GSDMD macrophages interacted with different types of immune cells, such as CD8+, CD4+ T, and Treg cells (Fig. 6, F and G).

DISCUSSION

The early diagnosis of sepsis remains challenging because of its complex etiology and lack of early clinical features (13). Therefore, it is essential to identify novel biomarkers that provide

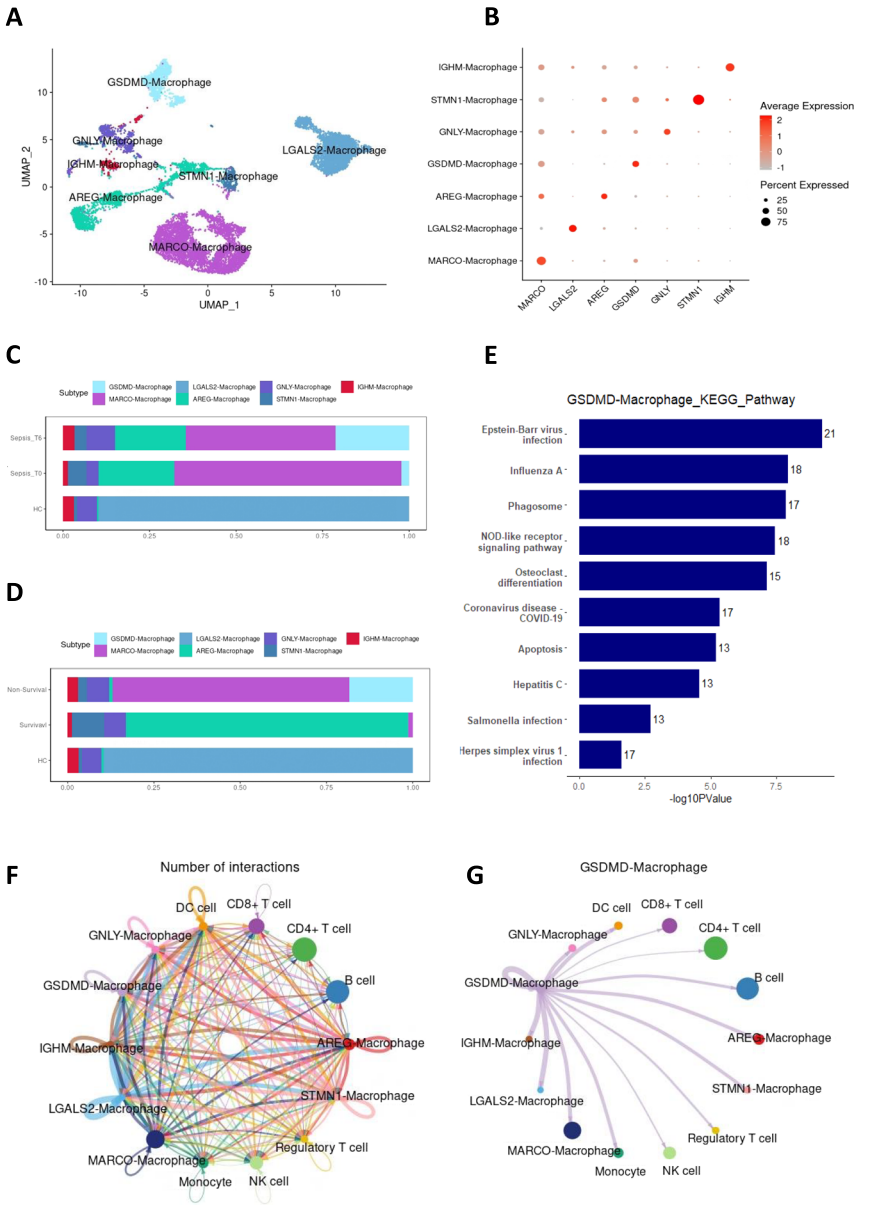

FIG. 6. **Subproportion analysis for PRGs related macrophage.** (A) The UMAP plot for subgroup of macrophage. (B) A dot plot showing the cell-specific marker gene expressions in subgroup of macrophage. (C) The percentage bar plot displayed the subgroup of macrophage composition in healthy controls and patients with sepsis, initially recognized and after 6 hours. (D) The percentage bar plot displayed the subgroup of macrophage composition in healthy controls and patients with different survival status. (E) A bar plot based on the top 10 KEGG enriched pathways for GSDMD-macrophage. (F) Overall communication condition of all cell clusters. Circle sizes are proportional to the number of cells in each cell group, and edge width represents the communication probability. (G) Communication condition between GSDMD-macrophage and other cell clusters. UMAP indicates uniform manifold approximation and projection; KEGG, Kyoto Encyclopedia of Genes and Genomes; PRG, pyroptosis-related genes; GSDMD, gasdermin D.

valuable insights. In this study, we used logistic LASSO regression to screen 10 PRGs associated with sepsis diagnosis, of which four were associated with the prognosis of sepsis. Multiple logistic regression models were constructed based on these genes, and their validity was verified using external cohorts. Our findings revealed two subtypes of sepsis associated with pyroptosis based on the different performances of the 10 genes in the sepsis samples. Subtype 2 had a poorer prognosis than subtype 1. Furthermore, functional enrichment analysis indicated that DEGs in subtypes 1 and 2 were associated with pyroptosis and immune-related pathways. The immune infiltration analysis revealed significant differences in the immune status between the two groups, with subtype 2 showing more severe immunosuppression. Using single-cell analysis, we found a subpopulation of macrophages characterized by GSDMD expression, which is involved in the pyroptosis-related pathway regulation and associated with the prognosis of patients with sepsis.

Pyroptosis is an immune response that plays a crucial role in the occurrence and development of sepsis (20). In the early stages of sepsis, the organism initiates pyroptosis to inhibit the intracellular replication of pathogens and accelerate their elimination (21). However, if the infection is not controlled, numerous pathogens invade the blood and cells to escape identification and elimination by the immune system (22). During this process, pathogen- and damage-associated molecular patterns are released, leading to massive pyroptosis, eventually causing organ failure and septic

shock (23,24). Therefore, pyroptosis may be associated with sepsis. Our diagnostic model, constructed based on 10 PRGs (*NLRP3*, *NAIP*, *GSDMD*, *GSDMB*, *ELANE*, *DPP9*, *DHX9*, *CASP4*, *CASP8*, and *APIP*), successfully distinguished patients with sepsis from healthy individuals. Among these, *DHX9*, *GSDMD*, *CASP4*, and *ELANE* are closely related to the prognosis of patients with sepsis.

RNA helicase DHX9 is a member of the human RNA enzyme family. Through DHX9, NLRP9b recognizes short double-stranded RNA stretches and forms inflammasome complexes with caspase-1 to promote pyroptosis (25). Our results indicated that DHX9 expression was significantly lower in patients with sepsis and that higher DHX9 expression was associated with a better prognosis. Because of the limited number of studies, the role of DHX9 in sepsis remains unclear, and our study may provide insights for future studies. Gasdermin D, an executor of pyroptosis, is an important downstream molecule that mediates pyroptosis in various lethal polymicrobial sepsis (13). Recent studies have shown that bacterial endotoxins induce disseminated intravascular coagulation in sepsis by activating the coagulation cascade through GSDMD-dependent phosphatidylserine exposure (26). Gasdermin D inhibition prevents multiple organ dysfunction during sepsis by blocking NET formation (27). Gasdermin D has also been shown to have protective effects against bacterial sepsis. The GSDMD-NT fragment released by GSDMD cleavage directly kills bacteria (28,29). Our results showed that GSDMD expression was upregulated in patients with sepsis and that patients with higher GSDMD expression had a better prognosis, which may be related to the direct bactericidal effect of GSDMD. However, there may be differences in the role of GSDMD in sepsis caused by endotoxins and bacterial sepsis that warrant further investigation. As a member of the caspase family, caspase-4 cleaves GSDMD via noncanonical inflammasome signaling (30), leading to pyroptosis. Our findings suggest that CASP4 shares the same expression pattern as GSDMD; that is, patients with poor prognoses had lower caspase-4 expression, which is consistent with previous findings (31). *ELANE* encodes neutrophil elastase, which is secreted by the neutrophils. Neutrophil elastase cleaves GSDMD and induces caspase-independent neutrophil pyroptosis (32). *ELANE* levels have been reported to correlate with the severity of sepsis (33). Our study showed that *ELANE* was upregulated significantly during sepsis and that was closely associated with a poor prognosis. We found that the majority of PRGs expression was downregulated in the sepsis subtype with a poor prognosis, suggesting that *ELANE* function was critical for severe sepsis.

Functional enrichment analysis revealed that poor prognostic subtypes of sepsis exhibit decreased activity of NOD-like receptor signaling and enhanced NET formation, a specific type of neutrophil cell death (34). Excessive NETs have been suggested to be critical players in the development of organ failure during sepsis (27), which may explain the different prognoses of the two subtypes. We further analyzed the expression patterns of key PRGs in neutrophils during sepsis, which indicated that both GSDMD and ELANE, key molecules involved in NETosis, are upregulated in patients with a poor prognosis. Therefore, it is reasonable to speculate that NET formation contributes to poor outcomes in patients with sepsis. Furthermore, this expression pattern suggests that ELANE-mediated neutrophil pyroptosis may be enhanced. However, the role of neutrophil pyroptosis in sepsis is unclear (35), and our study may provide insights for future studies. It is important to explore whether NETosis interacts with neutrophil pyroptosis to affect the prognosis of patients with sepsis.

The immune status of patients with sepsis may be a key factor in the disease's prognosis (36,37). Immune infiltration analysis revealed differences in immune-related pathways and immune cell composition between sepsis subtypes, with subtype 2 exhibiting more intense immunosuppression. This difference may explain the varying prognoses between the two subtypes. Sepsis-induced immunosuppression is characterized by the release of anti-inflammatory cytokines, immune cell death, T-cell exhaustion, and excessive production of immunomodulatory cells (38). Previous studies have shown that a large number of pyroptoses over a short period can lead to cellular expansion and lysis, causing intense inflammatory storms, organ dysfunction, and consequent immune cell failure (39). Our results show an increased proportion of Tregs in sepsis and subtype 2, as well as some key PRGs (*GADMD*, *CASP4*, and *DHX9*) that are closely correlated with Tregs. These findings suggest that Tregs may serve as a bridge between pyroptosis and immunosuppression.

Further single-cell analysis revealed significant changes in PRG expression in the early stages of sepsis. Initially, inflammatory and immune pathways in the patient's peripheral blood were robustly active; however, 6 hours later, the activity of these pathways decreased, whereas cell metabolic pathways such as oxidative phosphorylation, cholesterol homeostasis, and reactive oxygen pathways were gradually activated. This suggests that these immune cells may develop metabolic disorders and lose their immune functions, with an overall increase in PRG expression, indicating a gradual increase in pyroptosis. The regulation of immune cell pyroptosis has been shown to improve the prognosis of sepsis, with many studies focused on the regulation of macrophage pyroptosis (40). By further single-cell subpopulation analysis, we identified a macrophage subset based on GSDMD expression. Gasdermin D–expressing macrophages increased progressively with the development of sepsis and were only present in non-survivors of sepsis, suggesting a close association with poor prognosis. They can communicate with various immune cells, including Tregs, CD4+ T cells, and CD8+ T cells, and are associated with the NOD-like receptor pathway and apoptosis. Taking these results into consideration, we have reason to suspect that GSDMD-macrophage may regulate the immune status of septic patients through pyroptosis, thereby affecting the prognosis of septic patients.

Even though the combined scRNA-seq and bulk-seq analyses helped us understand PRG expression in sepsis and identify GSDMD macrophages, further mechanistic and experimental studies are required. This study had some limitations. First, it was a retrospective study, and prospective studies should be considered to avoid analytical bias. Second, this study was based on transcriptomics; however, both proteomic and spatial transcriptomic data need to be explored. Third, the prognostic factors in the GEO database were insufficient, with comorbidities and infectious microorganisms not included, and more complete cohorts are needed for validation.

In conclusion, we developed and validated a risk score for identifying sepsis based on 10 PRGs. Four of these also could be used to predict the diagnostic value in the prognosis of sepsis, and we identified a subset of GSDMD macrophages that may be associated with a poor prognosis. Our findings provide new

insights into the role of pyroptosis in sepsis and serve as a foundation for future studies.

REFERENCES

1. Singer M, Deutschman CS, Seymour CW, et al. The Third International Consensus Definitions for Sepsis and Septic Shock (Sepsis-3). *JAMA*. 2016;315(8):801–810.
2. Grondman I, Pirvu A, Riza A, et al. Biomarkers of inflammation and the etiology of sepsis. *Biochem Soc Trans*. 2020;48(1):1–14.
3. Font MD, Thyagarajan B, Khanna AK. Sepsis and septic shock — basics of diagnosis, pathophysiology and clinical decision making. *Med Clin North Am*. 2020; 104(4):573–585.
4. Cecconi M, Evans L, Levy M, et al. Sepsis and septic shock. *Lancet*. 2018; 392(10141):75–87.
5. Bauer M, Gerlach H, Vogelmann T, et al. Mortality in sepsis and septic shock in Europe, North America and Australia between 2009 and 2019 — results from a systematic review and meta-analysis. *Crit Care*. 2020;24(1):239.
6. van der Poll T, van de Veerdonk FL, Scicluna BP, et al. The immunopathology of sepsis and potential therapeutic targets. *Nat Rev Immunol*. 2017;17(7):407–420.
7. Vandewalle J, Libert C. Sepsis: a failing starvation response. *Trends Endocrinol Metab*. 2022;33(4):292–304.
8. Shi J, Gao W, Shao F. Pyroptosis: gasdermin-mediated programmed necrotic cell death. *Trends Biochem Sci*. 2017;42(4):245–254.
9. Wei X, Xie F, Zhou X, et al. Role of pyroptosis in inflammation and cancer. *Cell Mol Immunol*. 2022;19(9):971–992.
10. Chen R, Zeng L, Zhu S, et al. cAMP metabolism controls caspase-11 inflammasome activation and pyroptosis in sepsis. *Sci Adv*. 2019;5(5):eaav5562.
11. Rathkey JK, Zhao J, Liu Z, et al. Chemical disruption of the pyroptotic pore-forming protein gasdermin D inhibits inflammatory cell death and sepsis. *Sci Immunol*. 2018; 3(26):eaat2738.
12. Bortolotti P, Faure E, Kipnis E. Inflammasomes in tissue damages and immune disorders after trauma. *Front Immunol*. 2018;9:1900.
13. Kang R, Zeng L, Zhu S, et al. Lipid peroxidation drives Gasdermin D-mediated pyroptosis in lethal polymicrobial sepsis. *Cell Host Microbe*. 2018;24(1):97–108.e4.
14. Tang Y, Wang X, Li Z, et al. Heparin prevents caspase-11-dependent septic lethality independent of anticoagulant properties. *Immunity*. 2021;54(3):454–467.e6.
15. Zheng X, Chen W, Gong F, et al. The role and mechanism of pyroptosis and potential therapeutic targets in sepsis: a review. *Front Immunol*. 2021;12:711939.
16. Chousterman BG, Swirski FK, Weber GF. Cytokine storm and sepsis disease pathogenesis. *Semin Immunopathol*. 2017;39(5):517–528.
17. Bauer R, Rauch I. The NAIP/NLRC4 inflammasome in infection and pathology. *Mol Aspects Med*. 2020;76:100863.
18. Hao Y, Hao S, Andersen-Nissen E, et al. Integrated analysis of multimodal single-cell data. *Cell*. 2021;184(13):3573–3587.e29.
19. Becht E, McInnes L, Healy J, et al. Dimensionality reduction for visualizing single-cell data using UMAP. *Nat Biotechnol*. 2018;1546–1696.
20. Esquerdo KF, Sharma NK, Brunialti MKC, et al. Inflammasome gene profile is modulated in septic patients, with a greater magnitude in non-survivors. *Clin Exp Immunol*. 2017;189(2):232–240.
21. Qu M, Wang Y, Qiu Z, et al. Necroptosis, pyroptosis, ferroptosis in sepsis and treatment. *Shock*. 2022;57(6):161–171.
22. Nolt B, Tu F, Wang X, et al. Lactate and immunosuppression in sepsis. *Shock*. 2018; 49(2):120–125.
23. Burdette BE, Esparza AN, Zhu H, et al. Gasdermin D in pyroptosis. *Acta Pharm Sin B*. 2021;11(9):2768–2782.
24. Aglietti RA, Dueber EC. Recent insights into the molecular mechanisms underlying pyroptosis and gasdermin family functions. *Trends Immunol*. 2017;38(4):261–271.
25. Zhu S, Ding S, Wang P, et al. Nlrp9b inflammasome restricts rotavirus infection in intestinal epithelial cells. *Nature*. 2017;546(7660):667–670.
26. Yang X, Cheng X, Tang Y, et al. Bacterial endotoxin activates the coagulation cascade through gasdermin D–dependent phosphatidylserine exposure. *Immunity*. 2019;51(6):983–996.e6.
27. Silva CMS, Wanderley CWS, Veras FP, et al. Gasdermin D inhibition prevents multiple organ dysfunction during sepsis by blocking NET formation. *Blood*. 2021; 138(25):2702–2713.
28. Yang C, Sun P, Deng M, et al. Gasdermin D protects against noninfectious liver injury by regulating apoptosis and necroptosis. *Cell Death Dis*. 2019;10(7):481.
29. Liu X, Zhang Z, Ruan J, et al. Inflammasome-activated gasdermin D causes pyroptosis by forming membrane pores. *Nature*. 2016;535(7610):153–158.
30. Kayagaki N, Stowe IB, Lee BL, et al. Caspase-11 cleaves gasdermin D for non-canonical inflammasome signalling. *Nature*. 2015;526(7575):666–671.
31. Wang L, Zhang J, Zhang L, et al. Significant difference of differential expression pyroptosis-related genes and their correlations with infiltrated immune cells in sepsis. *Front Cell Infect Microbiol*. 2022;12:1005392.
32. Kambara H, Liu F, Zhang X, et al. Gasdermin D exerts anti-inflammatory effects by promoting neutrophil death. *Cell Rep*. 2018;22(11):2924–2936.
33. Kumar S, Gupta E, Kaushik S, et al. Quantification of NETs formation in neutrophil and its correlation with the severity of sepsis and organ dysfunction. *Clin Chim Acta*. 2019;495:606–610.
34. Sollberger G, Choidas A, Burn GL, et al. Gasdermin D plays a vital role in the generation of neutrophil extracellular traps. *Sci Immunol*. 2018;3(26):eaar6689.
35. Zhang H, Chen Z, Zhou J, et al. NAT10 regulates neutrophil pyroptosis in sepsis via acetylating ULK1 RNA and activating STING pathway. *Commun Biol*. 2022;5(1):916.
36. Delano MJ, Ward PA. Sepsis-induced immune dysfunction: can immune therapies reduce mortality? *J Clin Invest*. 2016;126(1):23–31.
37. van der Poll T, Shankar-Hari M, Wiersinga WJ. The immunology of sepsis. *Immunity*. 2021;54(11):2450–2464.
38. Liu D, Huang SY, Sun JH, et al. Sepsis-induced immunosuppression: mechanisms, diagnosis and current treatment options. *Mil Med Res*. 2022;9(1):56.
39. Shao R, Lou X, Xue J, et al. Review: the role of GSDMD in sepsis. *Inflamm Res*. 2022;71(10–11):1191–1202.
40. Wen X, Xie B, Yuan S, et al. The "self-sacrifice" of immunecells in sepsis. *Front Immunol*. 2022;13:833479.